Pediatric Cardiology (2022) 43:207–217
https://doi.org/10.1007/s00246-021-02719-6

ORIGINAL ARTICLE

Right Ventricular–Pulmonary Arterial Coupling in Repaired Tetralogy of Fallot

Sabine CHENG[1] · Vivian Wing-Yi LI[1] · Edwina Kam-Fung SO[1] · Yiu-Fai CHEUNG[1]

Received: 22 June 2021 / Accepted: 25 August 2021 / Published online: 31 August 2021

Abstract

We assessed right ventricular (RV)–pulmonary arterial (PA) coupling in patients with repaired tetralogy of Fallot (TOF). Sixty patients (34 males) aged 18.6 ± 8.3 years at 14.8 ± 7.4 years after repair and 60 controls were studied. Two-dimensional, tissue Doppler and speckle tracking echocardiography and colour flow mapping were performed to assess RV end-systolic (ESA) and -diastolic areas, tricuspid valve Doppler and myocardial velocities, left ventricular (LV) and RV deformation and pulmonary (PR), tricuspid regurgitation (TR), respectively. The ratios of RV area change to ESA and peak tricuspid annular systolic (*s*) velocity to RV ESA indexed to body surface area reflected RV–PA coupling. Patients had greater RV areas and reduced tricuspid annular and myocardial velocities, LV and RV myocardial mechanics compared to controls (all $p < 0.05$). Both RV area change/ESA ratio and peak tricuspid annular *s* velocity/indexed RV ESA ratio were reduced in patients (all $p < 0.001$). Sixty-one and 100% of patients had, respectively, RV area change/ESA ratio and peak tricuspid annular *s* velocity/indexed RV ESA ratio < -2SD of controls. Indices of RV–PA coupling correlated positively with tricuspid myocardial velocities, LV and RV deformation and inversely with PR and TR (all $p < 0.05$). Multivariate analysis showed RV systolic strain rate, PR and TR as independent predictors of both RV–PA coupling indices, whilst age, gender and LV systolic strain were also predictors of peak tricuspid annular *s* velocity/indexed RV ESA ratio (all $p < 0.05$). In conclusion, RV–PA coupling is impaired and is associated with RV and LV mechanics and severity of PR and TR in patients with repaired TOF.

Keywords Tetralogy of fallot · Right ventricular–pulmonary arterial coupling · Echocardiography

Introduction

In repaired tetralogy of Fallot (TOF), the long-term cardiovascular morbidities and mortalities remain to be important issues of concern. In particular, the impact of chronic pulmonary regurgitation (PR) and right ventricular (RV) dysfunction on exercise capacity, cardiac arrhythmias and sudden cardiac death is well documented [1–3]. Assessment of functional perturbation of the right ventricle has hence been the focus of studies of patients after TOF repair [4, 5]. Performance of the subpulmonary right ventricle should, however, be interpreted in the context of the pulmonary arterial (PA) system that it supports. In repaired TOF patients, alterations of PA substrates that may increase RV afterload exist. These include residual branch PA stenosis on the macroscopic scale [6] and increased medionecrosis and fibrosis of pulmonary arterioles on a microscopic scale [7, 8]. The understanding of maladaptation of the subpulmonary right ventricle is repaired TOF patients would hence be incomplete without evaluation of its coupling to the PA circulation.

Right ventricular–PA coupling refers to the relationship between RV contractility and its afterload as offered by the PA circulation [9]. The prognostic importance of RV–PA coupling is increasingly recognized in patients with advancing stages of heart failure [10] and in those with PA hypertension [11]. Whilst assessment of RV–PA coupling historically required invasive cardiac catheterization for determination of the ratio of RV end-systolic elastance (Ees) to effective arterial elastance (Ea) [9], non-invasive echocardiographic indices of coupling have increasingly been utilized for its quantification [12–16]. These latter indices are based on the ratio of echocardiography-derived indices of RV systolic function to those of RV afterload. Examples

✉ Yiu-Fai CHEUNG
xfcheung@hku.hk

[1] Division of Paediatric Cardiology, Department of Paediatrics and Adolescent Medicine, Queen Mary Hospital, The University of Hong Kong, 102, Pokfulam Road, Hong Kong, People's Republic of China

include the ratio of RV area change to end-systolic area (ESA) [12–14] and the ratio of peak tricuspid systolic annular velocity (*s*) to RV ESA indexed to body surface area [14].

Given the alteration of pulmonary arterial substrate as described above [6–8], we hypothesize that RV–PA coupling may be altered in patients with repaired TOF. The present study aimed to interrogate, using two-dimensional and tissue Doppler echocardiography, RV–PA coupling in patients with repaired TOF and to explore factors associated with its alteration.

Methods

This is a retrospective study of the echocardiographic recordings of 60 patients with repaired TOF selected randomly from our congenital heart database and those of 60 age-matched healthy controls. The healthy controls included hospital staff, healthy siblings of patients and subjects attending the cardiac clinic with functional heart murmur, non-specific chest pain or palpitation and for which no underlying organic causes were identified. The following patient data were retrieved from case notes: type of operation performed, date and age at primary repair, the need for and type of reinterventions and occurrence of cardiac arrhythmias. The body height and weight of all subjects at the time of echocardiographic acquisitions were used for calculation of body surface area and body mass index. This study was approved by the Institutional Review Board of the University of Hong Kong/Hospital Authority Hong Kong West Cluster, Hong Kong. Informed consent had been obtained from all participants at the time of acquisition of echocardiographic images.

Echocardiographic assessment was performed using Vivid 7 ultrasound machine (General Electric, Vingmed, Horton, Norway). Data were stored digitally and analysed offline using the EchoPAC software version 201 (General Electric, Vingmed, Horten, Norway). The values of echocardiographic parameters from three cardiac cycles were averaged for statistical analysis.

From the parasternal short-axis view, the LV end-systolic and -diastolic dimensions were measured by M-mode echocardiography. The LV shortening fraction was calculated according to standard formula. From the apical four-chamber view, tricuspid annular peak systolic excursion (TAPSE) was also obtained through M-mode interrogation. From this view, the RV ESA and end-diastolic (EDA) areas were measured. Right ventricular area change was calculated as the difference between RV ESA and EDA. Right ventricular fractional area change (FAC) was then calculated as (RV area change/RV EDA) × 100%. Trans-tricuspid pulsed-wave Doppler imaging was performed from the apical four-chamber view to determine the peak early (E) and late (A) tricuspid valve Doppler velocities and E/A ratio. Tissue Doppler imaging was then performed with sample volume placed at the basal RV free wall-tricuspid annular junction to obtain the following RV indices: *s*, early (*e*) and late (*a*) diastolic myocardial tissue velocities and *e*/*a* ratio. Right ventricular isovolumic myocardial acceleration (IVA), a relatively load-independent index of respective RV systolic function, was measured. The right-sided E/*e* ratio was calculated to estimate RV filling pressure. Colour flow mapping was used to assess semi-quantitatively the severity of PR and tricuspid regurgitation (TR) [17]. For PR, the width of the origin and the depth of penetration of the jet into the RV outflow were used to quantify its severity (mild: thin jet with a narrow origin; moderate: intermediate jet size; wide broad origin with deeper penetration). For tricuspid regurgitation, the area of the colour flow jet was used to quantify its severity (mild: a small and narrow central jet; moderate: moderate central jet; severe: a large central jet or an eccentric jet that impinges on the atrial wall). Two-dimensional speckle tracking echocardiography was performed for quantification of global LV and RV longitudinal myocardial deformation from the apical four-chamber view as reported previously [18, 19]. Briefly, the entire contours of the left and right ventricles were traced to determine the global systolic longitudinal strain (GLS), systolic (SRs), early (SRe) and late diastolic (SRa) strain rates of the two ventricles.

Right ventricular–PA coupling was assessed by the calculation of the following two indices: RV area change/ESA ratio [12–14] and peak tricuspid annular *s* velocity/indexed RV ESA ratio [14]. The ratio of RV area change/ESA ratio a two-dimensional surrogate measure of the stroke volume/end-systolic volume ratio, which has been shown to identify RV maladaptation in pulmonary hypertension [12]. The peak tricuspid annular *s* velocity/indexed RV ESA ratio has also been shown to be a useful bedside surrogate assessment of RV–PA coupling in patients with stable and decompensated pulmonary hypertension and in experimental models with acute variation of PA pressure [14].

Results are presented as mean ± SD. Right ventricular areas were indexed by body surface areas. Absolute values of strain and strain rates are presented to facilitate interpretation and statistical analyses. Demographics, clinical variables, echocardiographic indices and RV–PA coupling parameters of the patients and controls were compared using unpaired Student's t test. For the whole cohort, Pearson's correlation analysis was performed to explore associations between RV–PA coupling indices and demographic and echocardiographic functional indices. Multiple linear regression analysis of the entire cohort was performed to identify significant correlates of RV–PA coupling indices. The following covariates were included: age, gender, LV and RV GLS and systolic and diastolic strain rates and severity of PR and TR. Receiver operating characteristic (ROC)

curves were generated to determine the cutoff of RV–PA coupling and other echocardiographic indices to discriminate between patients and controls. A p value < 0.05 was considered statistically significant. All statistical analyses were performed using IBM SPSS Statistics 26 (SPSS, Chicago, Illinois, USA).

Results

Sixty (34 males) repaired TOF patients aged 18.6 ± 8.3 years who underwent corrective surgery at 4.1 ± 2.7 years were studied at 14.8 ± 7.4 years after repair. All of the patients had transannular patch repair of the the RV outflow obstruction. Additional interventions after initial repair included pulmonary valve replacement in three patients, closure of residual ventricular septal defect in 1 and balloon pulmonary angioplasty in 1. One patient had atrial flutter and ventricular tachycardia and underwent successful radiofrequency ablation. Four patients had syndromal associations, including DiGeorge syndrome in 3 and Down syndrome in 1. A total of 60 (30 males) controls, aged 16.6 ± 7.0 years ($p = 0.14$) were studied. The body weight (45.7 ± 15.8 kg vs 50.5 ± 17 kg, p = 0.17), height (151.6 ± 17.6 cm vs 155.4 ± 21.4 cm, p = 0.28), body mass index (19.2 ± 3.8 kg/m^2 vs 20.3 ± 4.0 kg/m^2, p = 0.13) and body surface area (1.4 ± 0.3 m^2 vs 1.5 ± 0.4 m^2, $p = 0.10$) were similar between the two groups.

Table 1 summarizes the echocardiographic findings in patients and controls. Compared with controls, patients had a larger LV systolic dimension ($p = 0.002$) and lower LV fractional shortening, GLS and systolic and diastolic strain rates (all $p < 0.001$). With regard to RV indices, patients had significantly greater RV end-systolic and -diastolic areas, and lower TAPSE, RV FAC, tricuspid E wave velocity and E/A ratio (all $p < 0.05$). Tissue Doppler imaging revealed worse RV systolic and diastolic function as evidenced by the lower tricuspid annular *s*, *e* and *a* velocities, and RV IVA, and higher tricuspid A wave velocity, *e*/*a* ratio and E/*e* ratio (all $p < 0.05$). Speckle tracking echocardiography further showed significantly lower RV GLS and systolic and diastolic strain rates in patients compared with controls (all $p < 0.001$). Of the 60 patients, 37 (61.7%) had absent or mild and 23 (38.3%) had moderate-to-severe TR, whilst 8 (14.3%) had absent or mild and 52 (86.7%) patients had moderate-to-severe PR.

With regard to the RV–PA coupling parameters, patients had significantly lower RV area change/ESA ratio (0.58 ± 0.17 vs 0.88 ± 0.12, $p < 0.001$) and peak tricuspid annular *s* velocity/indexed RV ESA ratio (0.54 ± 0.18 m^{2}s^{-1} cm^{-1} vs 1.85 ± 0.33 m^{2}s^{-1} cm^{-1}, $p < 0.001$) compared with controls (Fig. 1). Based on the RV area change/ESA ratio, using a cut-off of 0.64 (-2SD of control value), 37 (61.7%) patients had evidence of abnormal RV–PA coupling. Based on RV peak tricuspid annular *s* velocity/indexed RV ESA ratio, the lower limit of normal was 1.19 m^{2}s^{-1} cm^{-1} (-2SD of control value), and all of the patients were found to have ratios below the lower limit of normal.

Receiver operating characteristic curves were generated to determine the cutoff of RV–PA coupling indices to discriminate patients from controls (Fig. 2). Table 2 shows that peak tricuspid annular *s* velocity/indexed RV ESA ratio had the greater area under the ROC curve. A peak tricuspid annular *s* velocity/indexed RV ESA ratio of 1.07 m^{2}s^{-1} cm^{-1} had a sensitivity of 100% and a specificity of 100% to discriminate patients from controls.

Table 3 summarizes the results of univariate and multivariate analyses of clinical and cardiac functional parameters associated with RV–PA coupling. Univariate analysis identified that both RV–PA coupling indices were associated positively with tricuspid systolic and diastolic annular velocities, RV IVA and LV and RV GLS and strain rates and negatively with tricuspid *e*/*a* ratio, severity of PR and TR (all $p < 0.05$). Stepwise multivariate analysis of the entire studied cohort revealed RV SRs and severity of PR and TR as significant independent correlates of both RV–PA coupling indices (all $p < 0.05$). Age at study ($p < 0.001$), gender ($p = 0.024$), LV GLS ($p < 0.001$) and SRe were additionally identified as significant independent correlates of peak tricuspid annular *s* velocity/indexed RV ESA ratio (Fig. 3).

Discussion

The present study provides evidence of impaired RV–PA coupling in patients with repaired TOF, as reflected by the reduced RV area change/ESA and peak tricuspid annular *s* velocity/indexed RV ESA ratios. Indices of RV–PA coupling were found to correlate positively with parameters of RV and LV systolic and diastolic function and negatively with severity of PR and TR. To our knowledge, this is the first study to explore the relationships between RV–PA coupling parameters and RV and LV mechanics and severity of right-sided valvar regurgitation in patients with repaired TOF.

Whilst invasive cardiac catheterization with derivation of the RV Ees/Ea ratio remains to be the gold standard in the evaluation of RV–PA coupling, non-invasive echocardiographic evaluation of RV–PA coupling has increasingly been adopted for use in different clinical settings [10–16]. In this study, we determined RV–PA coupling by derivation of the RV area change/ESA and peak tricuspid annular *s* velocity/indexed RV ESA ratios [12–14]. These indices have been shown to correlate with invasively measured RV–PA coupling in animal [14] and clinical [12] studies. Both of these indices have been found to be reduced in adults with PA hypertension [13, 14]. Importantly, reduced peak tricuspid

Table 1 Echocardiographic indices of patients and controls

	TOF ($n=60$)	Controls ($n=60$)	p
Left ventricular indices			
M-mode echocardiography			
LV EDd (mm/m^2)	32.5 ± 8.0	30.4 ± 7.0	0.13
LV ESd (mm/m^2)	22.0 ± 5.8	19.1 ± 4.2	0.002*
FS (%)	32.5 ± 4.0	37.2 ± 4.4	< 0.001*
Longitudinal deformation			
Systolic strain (%)	15.5 ± 1.7	19.0 ± 1.6	< 0.001*
SRs (/s)	0.93 ± 0.15	1.10 ± 0.16	< 0.001*
SRe (/s)	1.67 ± 0.40	2.08 ± 0.43	< 0.001*
SRa (/s)	0.48 ± 0.14	0.60 ± 0.15	< 0.001*
Right ventricular indices			
M-mode echocardiography			
TAPSE (mm)	17.3 ± 1.5	24.6 ± 2.0	< 0.001*
2D echocardiography			
RV end-diastolic area (cm^2/m^2)	22.3 ± 6.6	11.0 ± 1.9	< 0.001*
RV end-systolic area (cm^2/m^2)	14.3 ± 4.7	5.9 ± 1.1	< 0.001*
Fractional area change (%)	36.0 ± 6.8	46.5 ± 3.5	< 0.001*
Tricuspid inflow Doppler indices			
E (cm/s)	54.2 ± 11.7	59.0 ± 13.5	0.040*
A (cm/s)	46.4 ± 12.5	31.7 ± 6.6	< 0.001*
E/A ratio	1.3 ± 0.4	1.9 ± 0.4	< 0.001*
Tricuspid annular tissue Doppler imaging			
s (cm/s)	7.1 ± 1.3	10.6 ± 1.0	< 0.001*
e (cm/s)	10.4 ± 2.0	13.1 ± 1.9	< 0.001*
a (cm/s)	4.3 ± 1.7	7.0 ± 2.7	< 0.001*
e/a ratio	2.8 ± 0.9	2.1 ± 0.8	< 0.001*
E/e ratio	5.4 ± 1.5	4.6 ± 1.2	0.001*
IVA (m/s^2)	0.4 ± 0.2	1.9 ± 0.4	< 0.001*
Longitudinal deformation			
Systolic strain (%)	16.5 ± 1.6	22.4 ± 3.0	< 0.001*
SRs (/s)	0.82 ± 0.15	1.29 ± 0.25	< 0.001*
SRe (/s)	1.29 ± 0.24	1.87 ± 0.46	< 0.001*
SRa (/s)	0.44 ± 0.22	0.75 ± 0.20	< 0.001*
Valvar regurgitation			
TR (nil-to-mild/moderate-to-severe)	37/23	60/0	< 0.001*
PR (nil-to-mild/moderate-to-severe)	8/52	60/0	< 0.001*

A late diastolic tricuspid inflow velocity, *a* tricuspid annular late diastolic velocity, *E* early diastolic tricuspid inflow velocity, *e* tricuspid annular early diastolic velocity, *EDd* end-diastolic internal dimension, *ESd* end-systolic internal dimension, *FS* shortening fraction, *IVA* isovolumic myocardial acceleration, *LV* left ventricular, *PR* pulmonary regurgitation, *RV* right ventricular, *s* peak tricuspid annular systolic velocity, *SRa* late diastolic strain rate, *SRe* early diastolic strain rate, *SRs* systolic strain rate, *TAPSE* tricuspid annular peak systolic excursion, *TR* tricuspid regurgitation

*Statistically significant

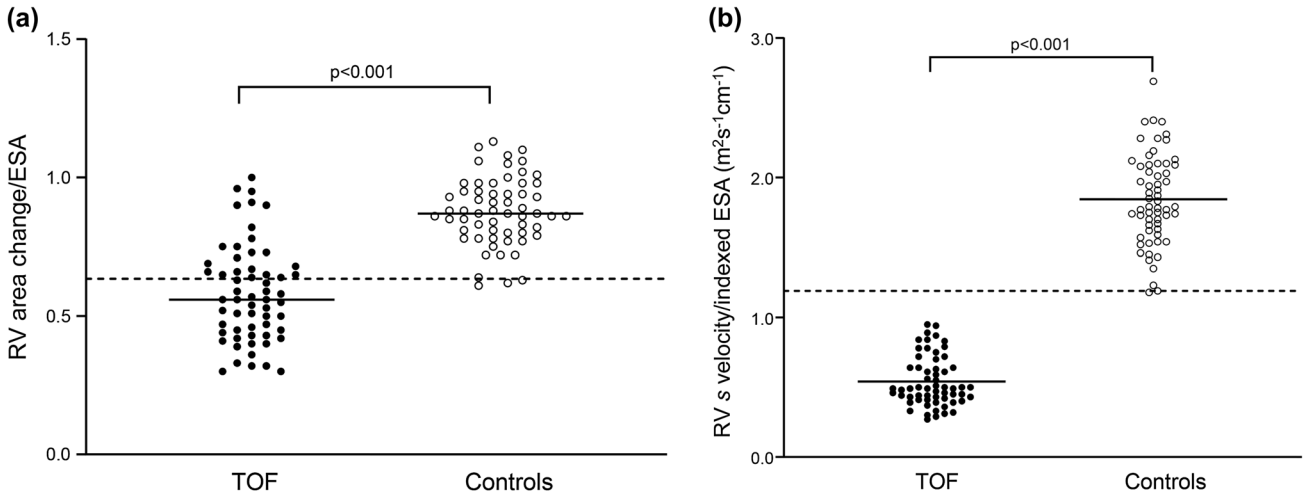

Fig. 1 Scatter plots showing (**a**) RV area change/ESA ratio and (**b**) peak tricuspid annular *s* velocity/indexed RV ESA ratio in patients and controls. Solid lines represent the mean of respective groups. Dashed lines represent the cutoff of 2 standard deviations below the mean of RV area change/ESA ratio and peak tricuspid annular *s* velocity/indexed RV ESA ratio of controls. *ESA* end-systolic area, *RV* right ventricular, *s* peak tricuspid annular systolic velocity

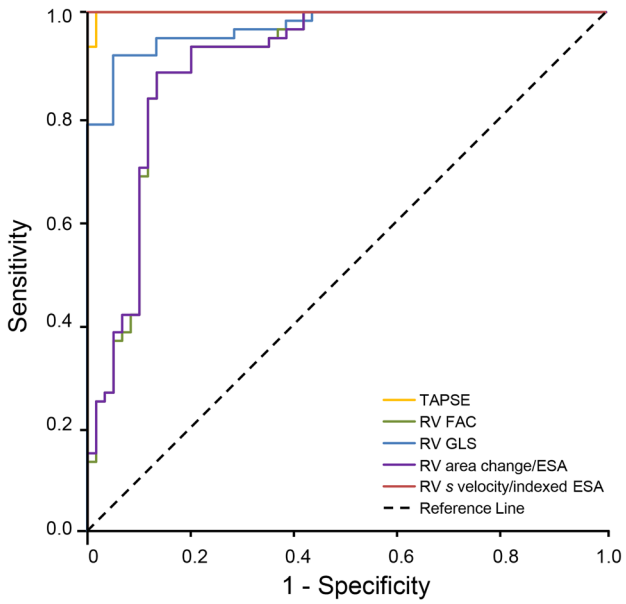

Fig. 2 Receiver operating characteristic curves for RV–PA coupling and RV systolic functional indices to discriminate between patients and controls. The dashed line is the reference line. *ESA* end-systolic area, *FAC* fractional area change, *GLS* global longitudinal strain, *RV* right ventricular, *s* peak tricuspid annular systolic velocity, *TAPSE* tricuspid annular peak systolic excursion

annular *s* velocity/indexed RV ESA ratio has been shown to predict mortality and the need for lung transplantation in patients with PA hypertension [14]. The RV area change/ESA ratio is a two-dimensional surrogate measure of RV stroke volume/end-systolic volume ratio, the latter being regarded as a simplified measure of the ventriculoarterial coupling ratio Ees/Ea [12–14]. Indeed, the ratio of magnetic resonance-derived RV stroke volume to end-systolic volume has been used to estimate Ees/Ea in TOF patients post repair [20, 21]. The use of these indices also obviates the need to measure RV systolic pressure, which is advantageous as some of the patients do not have TR for its estimation.

Our findings of significantly reduced RV area change/ESA ratio and peak tricuspid annular *s* velocity/indexed RV ESA ratio provide evidence of impaired RV–PA coupling in repaired TOF and agree with those reported previously. Latus et al. assessed the RV pressure–volume loops in a relatively small repaired TOF patient cohort and found that patients with transannular patch repair had worsening of RV–PA coupling during dobutamine stress [22]. Egbe et al. similarly found in adults with repaired TOF evidence of abnormal RV–PA coupling, the latter being also associated with exercise incapacity [15]. In this study, we further found that the coupling index of peak tricuspid annular *s* velocity/

Table 2 Area under the curve of right ventricular–pulmonary arterial coupling indices and right ventricular systolic functional indices

Parameter	Area under the curve	95% confidence interval	Cut-off value	Sensitivity (%)	Specificity (%)
RV area change/ESA	0.90	0.85–0.96	0.75	88.3	85.0
Peak tricuspid annular *s* velocity/indexed RV ESA	1.00	–	1.07	100.0	100.0

Abbreviations as shown in Table 1. *ESA* end-systolic area

indexed RV ESA ratio best discriminates patients from controls, as compared with parameters of systolic RV function and the RV area change/ESA ratio (Fig. 2). Interestingly, the value of peak tricuspid annular *s* velocity/indexed RV ESA ratio in our healthy controls, 1.85 ± 0.33, is numerically similar to the optimal RV Ees/Ea ratio of 1.5–2 [23]. The potential superiority of this RV–PA coupling index may perhaps be related to the inclusion of *s* velocity that reflects RV systolic function and RV ESA that reflects in a composite manner, indices of preload (end-diastolic volume), systolic function (Ees and ejection fraction) and ventricular-arterial coupling [24]. On the other hand, volume or area-based ratios of ventricular-vascular coupling have been regarded as ejection fraction in disguise [25]. Our finding of overlapping ROC curves of RV FAC and RV area change/ESA ratio (Table 2 and Fig. 2) supports this proposition.

Several factors contribute to impairment of RV–PA coupling in patients with repaired TOF. Geometric distortion and cardiac remodelling of the right ventricle secondary to chronic volume load alters RV contractile patterns and promotes RV–PA uncoupling [26, 27]. This is supported by our finding of strong negative associations between severity of PR and the RV–PA coupling indices and previous studies showing associations between impaired RV–PA coupling and RV dilation and systolic dysfunction [20, 28]. Furthermore, increased RV afterload may occur in our patients as a result of alteration of elastic architecture, increased medionecrosis, fibrosis found in the pulmonary arteries [7, 8]. Indeed, Inuzuka et al. have found reduced PA compliance with greater PA pressure wave reflection and RV end-diastolic volume in children with repaired TOF [29]. Reduced PA compliance also increases PR to increase RV preload [30]. Additionally, the present study suggests that impairment of LV systolic and diastolic myocardial deformation may lead to unfavourable RV–PA coupling. Our findings corroborate those of Buddhe et al. who found that reduced LV ejection was associated with abnormal RV end-systolic volume/stroke volume ratio in adolescents with repaired TOF [28]. It is probable that LV dysfunction may increase RV afterload through reducing PA compliance and increasing pulmonary vascular resistance [31].

An intriguing novel finding of the present study is the association between severe TR and worse RV–PA coupling after TOF repair. In adults with heart failure with reduced ejection fraction, the presence and severity of TR has recently been shown to be associated with RV–PA uncoupling [32]. In patients with secondary TR, RV–PA uncoupling was the only echocardiographic parameter independently associated with all-cause mortality [33]. Whether TR is a manifestation or surrogate of severity of impaired RV–PA coupling, or a contributor of worsening RV–PA uncoupling is, however, unclear. In patients with repaired TOF, this novel finding should prompt further studies to determine the possible mechanisms and pathophysiological implications.

Table 3 Correlates of right ventricular–pulmonary arterial coupling indices

	RV area change/ESA				Peak tricuspid annular *s* velocity/indexed RV ESA			
	r	*p*	*β*	*p*	*r*	*p*	*β*	*p*
Demographics								
Age	− 0.17	0.07	0.81	0.93	0.05	0.56	0.21	< 0.001*
Gender	0.12	0.21	0.30	0.99	0.002	0.98	− 0.09	0.024*
Left ventricular indices								
Longitudinal deformation								
Systolic strain	0.55	< 0.001*	0.16	0.51	0.69	< 0.001*	0.30	< 0.001*
SRs	0.40	< 0.001*	0.45	0.69	0.46	< 0.001*	0.26	0.31
SRe	0.43	< 0.001*	0.23	0.64	0.36	< 0.001*	− 0.13	0.039*
SRa	0.27	0.003*	− 0.11	0.80	0.40	< 0.001*	0.73	0.69
Right ventricular indices								
Tricuspid annular tissue Doppler imaging								
s	0.53	< 0.001*	–	–	0.84	< 0.001*	–	–
e	0.37	< 0.001*	–	–	0.58	< 0.001*	–	–
a	0.36	< 0.001*	–	–	0.59	< 0.001*	–	–
e/a ratio	− 0.20	0.028*	–	–	–0.39	< 0.001*	–	–
E/e ratio	− 0.16	0.10	–	–	–0.33	< 0.001*	–	–
IVA	0.64	< 0.001*	–	–	0.85	< 0.001*	–	–
Longitudinal deformation								
Systolic strain	0.58	< 0.001*	0.74	0.20	0.72	< 0.001*	0.08	0.19
SRs	0.60	< 0.001*	0.23	0.010*	0.70	< 0.001*	0.25	< 0.001*
SRe	0.48	< 0.001*	0.75	0.33	0.55	< 0.001*	0.88	0.31
SRa	0.44	< 0.001*	0.25	0.49	0.61	< 0.001*	0.42	0.47

Table 3 (continued)

	RV area change/ESA				Peak tricuspid annular *s* velocity/indexed RV ESA			
	r	*p*	*β*	*p*	*r*	*p*	*β*	*p*
Valvar regurgitation								
PR severity	− 0.68	< 0.001*	− 0.45	< 0.001*	− 0.83	< 0.001*	− 0.52	< 0.001*
TR severity	− 0.47	< 0.001*	− 0.16	0.038*	− 0.48	< 0.001*	− 0.11	0.019*

Abbreviations as shown in Table 1

*Statistically significant

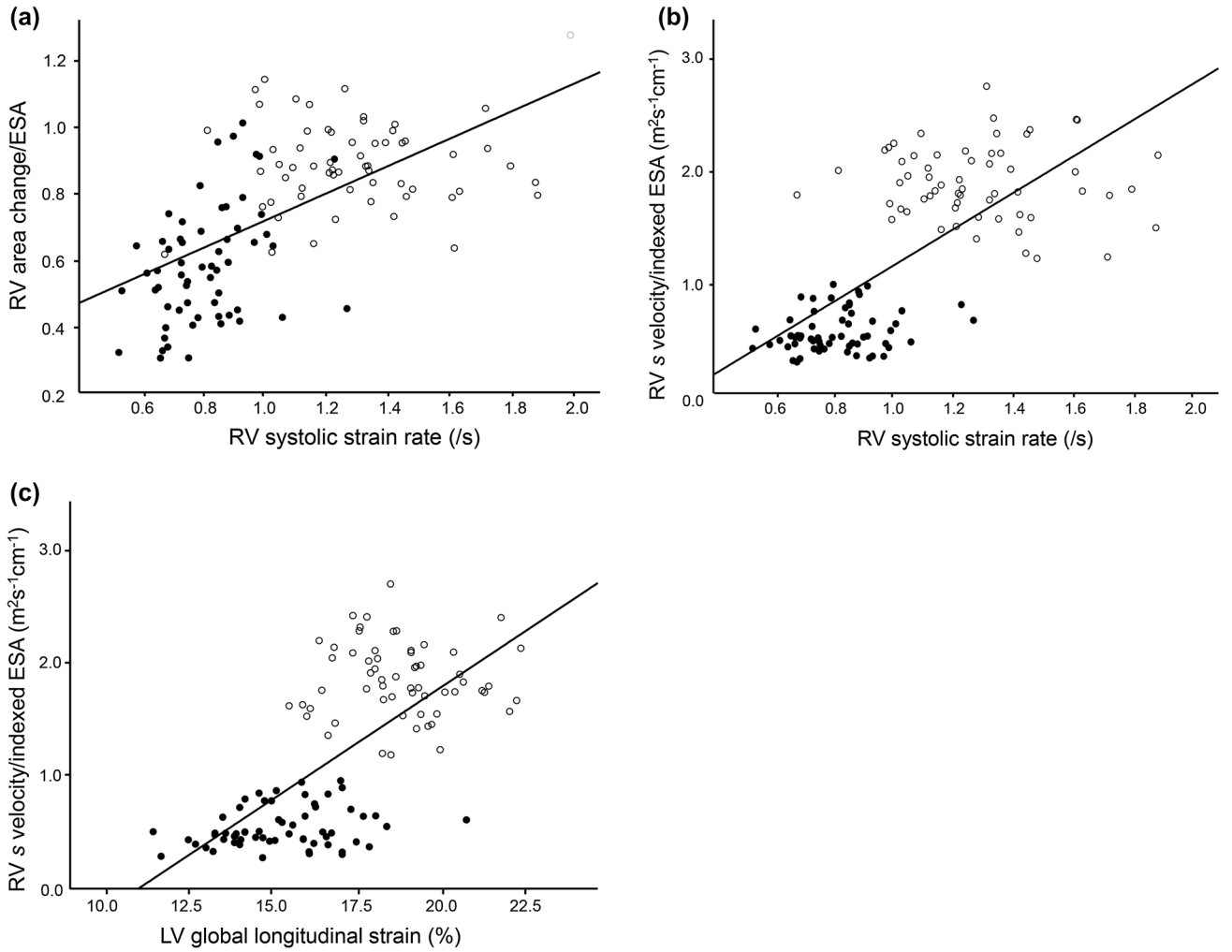

Fig. 3 Scatter plots showing correlations between (**a**) RV area change/ESA ratio and RV systolic strain rate, and (**b**) peak tricuspid annular *s* velocity/indexed RV ESA ratio and RV systolic strain rate and (**c**) peak tricuspid annular *s* velocity/indexed RV ESA ratio and LV GLS. Solid circles represent patients, empty circles represent controls. *ESA* end-systolic area, *LV* left ventricular, *RV* right ventricular, *s* peak tricuspid annular systolic myocardial velocity

Our findings of altered RV–PA coupling and its associations with altered RV and LV mechanics and right-sided valvar regurgitation have several clinical implications. First, the potential prognostic value of RV–PA coupling is shown by the recently reported association between cardiac magnetic resonance-derived RV–PA coupling index and the composite outcome of death, aborted sudden cardiac death, or sustained ventricular tachycardia in patients with repaired TOF [21]. Second, assessment of RV–PA coupling may provide incremental information on early detection of abnormal RV performance as uncoupling has been found in repaired TOF patients with normal TAPSE and RV FAC [16]. Third, our findings of associations between RV–PA coupling and severity of TR and PR should provide the basis for further discussions on the incorporation of RV–PA coupling indices when deciding the optimal timing of pulmonary valve replacement and necessity of tricuspid valve repair in repaired patients undergoing surgical implantation of the pulmonary valve.

Several limitations of the study warrant comments. This is a retrospective study that does not allow the determination of prognostic value of RV–PA coupling in repaired TOF. Longitudinal studies are required to evaluate the evolution of RV–PA coupling indices and their relationship to outcomes in repaired TOF patients. Larger scale prospective studies are required to establish the prognostic value of RV–PA uncoupling in these patients. We have explored only RV–PA coupling at rest in the present study. Given the reported associations between RV–PA coupling and exercise capacity [15, 16], it would be worthwhile to interrogate the changes on RV–PA coupling during exercise stress.

In conclusion, RV–PA coupling is impaired and is associated with RV and LV mechanics and severity of PR and TR

in patients with repaired TOF. Further studies to determine the prognostic significance of impaired RV–PA coupling in these patients are warranted.

Authors Contribution Sabine Cheng: Conceptualization, Methodology, Investigation, Formal analysis, Writing original draft. Vivian Wing-Yi Li: Conceptualization, Methodology, Writing–review & editing. Edwina Kam-Fung So: Formal analysis, Data curation. Yiu-Fai Cheung: Supervision, Conceptualization, Writing review & editing.

Funding This study did not receive any grant support.

Data availability Data generated by our study that supports the conclusion of our article are available from the corresponding author upon reasonable request for research use.

Declarations

Conflicts of interest All of the authors declare no conflict of interest.

Ethical Approval The review of clinical records, without additional procedures performed in patients and the need to obtain informed consent, was approved by the Institutional Review Board of the University of Hong Kong/Hospital Authority Hong Kong West Cluster, Hong Kong, China, and in accordance with the 1964 Helsinki declaration and its later amendments or comparable ethical standards.

Consent to Participate Previous consent has for echocardiographic recordings been obtained from all participants.

Consent for Publication Previous consent has been obtained from all participants.

References

1. Friedberg MK, Fernandes FP, Roche SL, Slorach C, Grosse-Wortmann L, Manlhiot C, Fackoury C, McCrindle BW, Mertens L, Kantor PF (2013) Relation of right ventricular mechanics to exercise tolerance in children after tetralogy of Fallot repair. Am Heart J 165:551–557
2. Gatzoulis MA, Balaji S, Webber SA, Siu SC, Hokanson JS, Poile C, Rosenthal M, Nakazawa M, Moller JH, Gillette PC, Webb GD, Redington AN (2000) Risk factors for arrhythmia and sudden cardiac death late after repair of tetralogy of Fallot: a multicenter study. Lancet 356:975–981
3. Apitz C, Webb GD, Redington AN (2009) Tetralogy of Fallot. Lancet 374:1462–1471
4. Yu HK, Li SJ, Ip JJ, Lam WW, Wong SJ, Cheung YF (2014) Right ventricular mechanics in adults after surgical repair of tetralogy of Fallot: insights from three-dimensional speckle-tracking echocardiography. J Am Soc Echocardiogr 27:423–429
5. Frigiola A, Redington AN, Cullen S, Vogel M (2004) Pulmonary regurgitation is an important determinant of right ventricular contractile dysfunction in patients with surgically repaired tetralogy of Fallot. Circulation 110: 153–157.
6. Maskatia SA, Spinner JA, Morris SA, Petit CJ, Krishnamurthy R, Nutting AC (2013) Effect of branch pulmonary artery stenosis on right ventricular volume overload in patients with tetralogy of Fallot after initial surgical repair. Am J Cardiol 111:1355–1360
7. Bédard E, McCarthy KP, Dimopoulos K, Giannakoulas G, Gatzoulis MA, Ho SY (2009) Structural abnormalities of the pulmonary trunk in tetralogy of Fallot and potential clinical implications: a morphological study. J Am Coll Cardiol 54:1883–1890
8. Chowdhury UK, Bishnoi AK, Ray R, Kalaivani M, Kapoor PM, Reddy SM, Mishra AK, Gonvindappa RM (2009) Central pulmonary artery histopathology in patients with cyanotic congenital heart diseases. Ann Thorac Surg 87:589–596
9. Bellofiore A, Chesler N (2013) Methods for measuring right ventricular function and hemodynamic coupling with the pulmonary vasculature. Ann Biomed Eng 41:1384–1398
10. Nochioka K, Querejeta Roca G, Claggett B, Biering-Sørensen T, Matsushita K, Hung CL, Solomon SD, Kitzman D, Shah AM (2018) Right ventricular function, right ventricular-pulmonary artery coupling, and heart failure risk in 4 US communities: the Atherosclerosis Risk in Communities (ARIC) study. JAMA Cardiol 3:939–948
11. Vanderpool RR, Pinsky MR, Naeije R, Deible C, Kosaraju V, Bunner C, Mathier MA, Lacomis J, Champion HC, Simon MA (2015) Right ventricular-pulmonary arterial coupling predicts outcome in patients referred for pulmonary hypertension. Heart 101:37–43
12. Tello K, Wan J, Dalmer A, Vanderpool R, Ghofrani HA, Naeije R, Roller F, Mohajerani E, Seeger W, Herberg U, Sommer N, Gall H, Richter MJ (2019) Validation of the tricuspid annular plane systolic excursion/systolic pulmonary artery pressure ratio for the assessment of right ventricular arterial coupling in severe pulmonary hypertension. Circ Cardiovasc Imaging 12:e009047
13. French S, Amsallem M, Ouazani N, Li S, Kudelko K, Zamanian RT, Haddad F, Chung L (2018) Non-invasive right ventricular load adaptability indices in patients with scleroderma-associated pulmonary arterial hypertension. Pulm Circ 8:2045894018788268
14. Boulate D, Amsallem M, Tatiana K, Zamanian RT, Fadel E, Mercier O, Haddad F (2019) Echocardiographic evaluations of right ventriculoarterial coupling in experimental and clinical pulmonary hypertension. Physiol Resp 7:e14322
15. Egbe AC, Kothapalli S, Miranda WR, Pislaru S, Ammash NM, Borlaug BA, Pellikka PA, Najam M, Connolly HM (2019) Assessment of right ventricular-pulmonary arterial coupling in chronic pulmonary regurgitation. Can J Cardiol 35:914–922
16. Egbe AC, Miranda WR, Pellikka PA, Pislaru SV, Borlaug BA, Kothapalli S, Ananthaneni S, Sandhyavenu H, Najam M, Farouk Abdelsamid M, Connolly HM (2019) Right ventricular and pulmonary vascular function indices for risk stratification of patients with pulmonary regurgitation. Congenit Heart Dis 14:657–664
17. Zoghbi WA, Adams D, Bonow RO, Enriquez-Sarano M, Foster E, Grayburn PA, Hahn RT, Han Y, Hung J, Lang RM, Little SH, Shah DJ, Shernan S, Thavendiranathan P, Thomas JD, Weissman NJ (2017) Recommendations for non-invasive evaluation of native valvular regurgitation: a report from the American Society of Echocardiography developed in collaboration with the Society for Cardiovascular Magnetic Resonance. J Am Soc Echocardiogr 30:303–371
18. Cheung EW, Liang XC, Lam WW, Cheung YF (2009) Impact of right ventricular dilation on left ventricular myocardial deformation in patients after surgical repair of tetralogy of Fallot. Am J Cardiol 104:1264–1270
19. Chow PC, Liang XC, Cheung EWY, Lam WWM, Cheung YF (2008) New two-dimensional global longitudinal strain and strain rate for assessment of right ventricular function. Heart 94:855–859
20. Sandeep B, Huang X, Li Y, Wang X, Mao L, Kan Y, Xiong D, Gao K, Zongwei X (2020) Evaluation of right ventricle pulmonary artery coupling on right ventricular function in post-operative tetralogy of Fallot patients underwent for pulmonary valve replacement. J Cardiothorac Surg 15:241

21. Godfrey ME, Geva T, Sleeper LA, Lu M, Valente AM, Prakash A (2016) Ventriculoarterial coupling ratio is associated with adverse outcome in repaired tetralogy of Fallot. Circulation 134(suppl):1
22. Latus H, Binder W, Kerst G, Hofbeck M, Sieverding L, Apitz C (2013) Right ventricular-pulmonary arterial coupling in patients after repair of tetralogy of Fallot. J Thorac Cardiovasc Surg 146:1366–1372
23. Tello K, Dalmer A, Axmann J, Vanderpool R, Ghofrani HA, Naeije R, Roller F, Seeger W, Sommer N, Wilhelm J, Gall H, Richter MJ (2019) Reserve of right ventricular-arterial coupling in the setting of chronic overload. Circ Heart Fail 12:e005512
24. Kerkhof PLM, Kuznetsova T, Ali R, Handly N (2018) Left ventricular volume analysis as a basic tool to describe cardiac function. Adv Physiol Educ 42:130–139
25. Namasivayam M, Hayward CS, Muller DWM, Jabbour A, Feneley MP (2019) Ventricular-vascular coupling ratio is the ejection fraction in disguise. J Am Soc Echocardiogr 32:791
26. Carlsson M, Ugander M, Heiberg E, Arheden H (2007) The quantitative relationship between longitudinal and radial function in left, right, and total heart pumping in humans. Am J Physiol Heart Circ Physiol 293:H636-644
27. Sheehan FH, Ge S, Vick GW 3rd, Urnes K, Kerwin WS, Bolson EL, Chung T, Kovalchin JP, Sahn DJ, Jerosch-Herold M, Stolpen AH (2008) Three-dimensional shape analysis of right ventricular remodeling in repaired tetralogy of Fallot. Am J Cardiol 101:107–113
28. Buddhe S, Jani V, Sarikouch S, Gaur L, Schuster A, Beerbaum P, Lewin M, Kutty S (2021) Differences in right ventricular-pulmonary vascular coupling and clinical indices between repaired standard tetralogy of Fallot and repaired tetralogy of Fallot with pulmonary atresia. Diagn and Intervl Imaging 102:85–91
29. Inuzuka R, Seki M, Sugimoto M, Saiki H, Masutani S, Senzaki H (2013) Pulmonary arterial wall stiffness and its impact on right ventricular afterload in patients with repaired tetralogy of Fallot. Ann Thorac Surg 96:1435–1441
30. Kilner PJ, Balossino R, Dubini G, Babu-Narayan SV, Taylor AM, Pennati G, Migliavacca F (2009) Pulmonary regurgitation: the effects of varying pulmonary artery compliance, and of increased resistance proximal or distal to the compliance. Int J Cardiol 133:157–166
31. Dupont M, Mullens W, Skouri HN, Abrahams Z, Wu Y, Taylor DO, Starling RC, Tang WH (2012) Prognostic role of pulmonary arterial capacitance in advanced heart failure. Circ Heart Fail 5:778–785
32. Schmeisser A, Rauwolf T, Groscheck T, Tanev I, HansenM MS, Steendijk P, Braun-Dallaeus, (2020) Right ventricular pulmonary vascular coupling in secondary tricuspid regurgitation: a pressure volume loop study. Eur Heart J 41(ehaa946):1903
33. Fortuni F, Butcher SC, Dietz MF, van der Bijl P, Prihadi EA, De Ferrari GM, Marsan NA, Bax JJ, Delgado V (2021) Right ventricular-pulmonary arterial coupling in secondary tricuspid regurgitation. Am J Cardiol S0002–9149(21):00212–00215